Progress In Electromagnetics Research, PIER 97, 391–405, 2009

A NOVEL ELECTRONIC BEAM STEERING TECHNIQUE IN TIME MODULATED ANTENNA ARRAYS

G. Li, S. Yang, Y. Chen, and Z. Nie

Department of Microwave Engineering
School of Electronic Engineering
University of Electronic Science and Technology of China (UESTC)
Chengdu 610054, China

Abstract—In this paper, a novel technique for electronic beam steering in time modulated linear array (TMLA) is proposed. The beam steering technique is realized at the first sideband by controlling the switch-on time sequences of each element in the TMLA without using phase shifters. The differential evolution (DE) algorithm is employed to improve the gain and suppress the sidelobe levels (SLLs) at both the center frequency and the first sideband, simultaneously. An *S*-band 8-element double-layered printed dipole linear array was used to verify the technique experimentally. Measured results are compared with numerical data, and good agreement is reported. Moreover, some simulation results on the binary phase shift keying (BPSK) modulated signals arriving from different directions received by the proposed approach are presented, which validates the application of the proposed beam steering technique.

1. INTRODUCTION

Electronic beam steering is the key issue in phased arrays widely used in military and commercial applications including radar systems and wireless communications. Many studies have been carried out for the electronic beam steering, and the most popular method is the use of phase shifters. Being the general devices used in phased arrays, phase shifters are critical components especially in transmit/receive modules due to the fact that phase shifters can produce phase shifts between elements of antenna arrays and steer the beam to the desired direction. However, the cost of phase shifters is usually up to nearly half of the cost of an entire electronically scanned phased array. In addition, most

Corresponding author: S. Yang (swnyang@uestc.edu.cn).

of the widely used GaAs based semiconductor phase shifters usually have very high insertion loss up to 13 dB or even more. Consequently, it is attractive to study some new techniques for electronic beam steering.

On the other hand, the time modulated antenna arrays (TMAAs) were firstly proposed as a means of synthesizing low/ultra-low sidelobe patterns by using RF switches to control the antenna elements [1]. As compared to conventional antenna arrays, the time modulated antenna arrays introduce a fourth dimension -time- into the design, and the time parameter used to taper the distribution can be easily, rapidly and accurately adjusted. Consequently, TMAAs have more flexibility for the design. Due to the time modulation that the TMAAs generate unwanted sidebands spaced at multiples of the time modulation frequency, which may cause the energy losses. Some studies on minimizing sideband level (SBL) were proposed in [2–5]. However, sidebands are not always harmful to the TMAAs. H. E. Shanks proposed a simultaneous scan operation based on time modulation technology where the beams at different sidebands were used to point at different directions [6]. A two-element TMAA with direction finding properties was proposed in [7] where the electronic null scanning can be realized at the first sideband by adjusting switching times of the both elements.

In this paper, a novel electronic beam steering technique in time modulated linear arrays (TMLAs) is proposed and studied. This technique is carried out at the first sideband without using phase shifters in the array. By adjusting the switch-on time instant of each element in one time modulation period, the electronic beam steering can be realized. Moreover, by controlling the switch-on time intervals of each element, desired patterns can be synthesized. The differential evolution (DE) algorithm is employed to suppress the SLLs at the center frequency and the first sidebands and to improve the gain simultaneously. The application of the proposed beam steering technique is also studied and some simulation results on binary phase shift keying (BPSK) modulated signals arriving from different directions received by the proposed approach are presented.

2. THEORY

In this section, the theory of the novel electronic beam steering technique is presented and the DE algorithm is also introduced.

2.1. Electronic Beam Steering Technique

Let us consider an N-element linear array of equally spaced isotropic elements. Suppose that each element is connected with a RF switch, the array factor of the TMLA is given by [2]

$$F(\theta, t) = e^{j2\pi f_0 t} \sum_{k=1}^{N} A_k e^{j\alpha_k} U_k(t) \cdot e^{j(k-1)\beta d \sin\theta} \tag{1}$$

where f_0 is the center frequency of the array, A_k and α_k are the static excitation amplitude and phase of the kth element, respectively, d is the element spacing of the array, $\beta = 2\pi f_0/c$, c is the velocity of light in free space, θ denotes the angle measured from the broadside direction of the array. As shown in Fig. 1, the time switching function $U_k(t)$ for the kth element is given by

$$U_k(t) = \begin{cases} 1, & t_{0k} \le t \le t_{0k} + \tau_k \\ 0, & \text{otherwise} \end{cases} \tag{2}$$

where t_{0k} is the switch-on time instant and τ_k is the duration of "on" times. Due to the periodicity of $U_k(t)$, the space and frequency response of (1) can be obtained by decomposing it into Fourier series, and each frequency component has a frequency of n/T_p ($n = 0, \pm1, \pm2, \ldots, \pm\infty$), where T_p is the time modulation period. The nth order Fourier component can be written as

$$F_n(\theta, t) = e^{j2\pi(f_0 + nf_p)t} \sum_{k=1}^{N} a_{nk} \cdot e^{j(\varphi_k + \alpha_k)} \tag{3}$$

where $f_p = 1/T_p$, $\varphi_k = (k-1)\beta d \sin\theta$ and a_{nk} is the complex amplitude and is given by

$$a_{nk} = A_k f_p \tau_k \frac{\sin(n\pi f_p \tau_k)}{n\pi f_p \tau_k} e^{-jn\pi f_p (2t_{0k} + \tau_k)}. \tag{4}$$

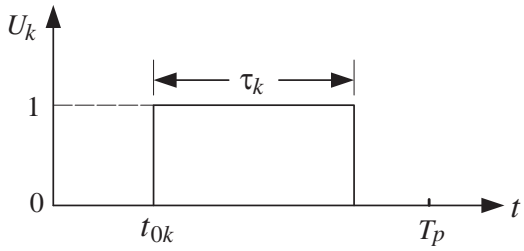

Figure 1. Scheme of the time switching function.

τ_k and t_{0k} can be normalized in one time modulation period T_p. Thus, according to (3) and (4), the array factor of the TMLA at the center frequency ($n = 0$), the first positive sideband ($n = 1$) and the first negative sideband ($n = -1$) can be written as (5)–(7), respectively, given by

$$F_0(\theta, t) = e^{j2\pi f_0 t} \sum_{k=1}^{N} A_k \xi_k e^{j(\varphi_k + \alpha_k)} \tag{5}$$

$$F_1(\theta, t) = \frac{e^{j2\pi(f_0+f_p)t}}{\pi} \sum_{k=1}^{N} A_k \sin(\pi\xi_k)\, e^{-j\pi(2\upsilon_k+\xi_k)} e^{j(\varphi_k+\alpha_k)} \tag{6}$$

$$F_{-1}(\theta, t) = \frac{e^{j2\pi(f_0-f_p)t}}{\pi} \sum_{k=1}^{N} A_k \sin(\pi\xi_k)\, e^{j\pi(2\upsilon_k+\xi_k)} e^{j(\varphi_k+\alpha_k)} \tag{7}$$

where $\xi_k = \tau_k/T_p$ and $\upsilon_k = t_{0k}/T_p$. By observing (5), the direction of the main beam at f_0 is only dependent on α_k, whereas, due to the term $e^{-j\pi(2\upsilon_k+\xi_k)}$ in (6), the array factor of the TMLA at the $f_0 + f_p$ has phase shift between elements. In (6), in order to make $\sin(\pi\xi_k)$ vary in the range [0, 1], ξ_k should be in the range [0, 0.5] and υ_k should be varied in the range [−0.5, 0.5] to make sure that the phase shift is in the range $[-\pi, \pi]$. To synthesize desired patterns at $f_0 + f_p$, let $g_k = A_k \sin(\pi\xi_k)$, and g_k can be a certain distribution such as Chebyshev and Taylor distribution. Thus, ξ_k can be obtained by

$$\xi_k = \frac{1}{\pi} \arcsin\left(\frac{g_k}{A_k}\right). \tag{8}$$

Suppose that the desired beam pointing at $f_0 + f_p$ is θ_0, (6) will have its maximum at the desired angle $\theta = \theta_0$ when

$$\upsilon_k = \frac{1}{2}\left[\frac{\alpha_k + (k-1)\,\beta d \sin\theta_0}{\pi} - \xi_k\right]. \tag{9}$$

Thus, the desired patterns can be synthesized and the electronic beam steering can be realized by using (8) and (9). Moreover, the relationship of directions of the three beams at f_0 and $f_0 \pm f_p$ can be obtained from (5)–(7), which is that the beam at $f_0 - f_p$ will be located at $2\theta_{f_0} - \theta_0$ when the direction of the beam at f_0 is at θ_{f_0}. With the proposed time sequences for the electronic beam scanning, the way of calculation for the directivity and gain of the TMLA is similar to that proposed in [8]. The simulated and measured results on patterns and gains will be presented in Section 4.

2.2. Differential Evolution Algorithm

The DE is a type of evolution algorithm which can be used to perform global optimization and operates on the so-called three kinds of operators, namely, mutation, crossover and selection, which are quite different from those in genetic algorithm. The DE has already been proven to be an efficient optimization approach in areas such as electromagnetic inverse scattering [9], array pattern synthesis [10], and some design problems [11–13].

In order to improve the gain as high as possible and suppress the SLLs of the TMLA, the DE algorithm is adopted to optimize the time sequences of each element. For the purpose of simplification in the analysis, the static amplitude distribution A_k is selected as uniform. Thus, the optimization parameter vector is $v = \{\tau_k\}$ and the cost function is selected as

$$\begin{aligned} f^{(n)}(v) &= w_1 \cdot \left(SLL^{(n)}_{\max}(v)\,|_{f_0} - SLL_0 \right) \\ &\quad + w_2 \cdot \left(SLL^{(n)}_{\max}(v)\,|_{f_0+f_p} - SLL_1 \right) \\ &\quad + w_3 \cdot G^{(n)}_{\max}(v)\,|_{f_0} + w_4 \cdot G^{(n)}_{\max}(v)\,|_{f_0+f_p} \end{aligned} \tag{10}$$

where $SLL_{\max}$ is the simulated maximum SLL, SLL_0 and SLL_1 are the specified SLLs at f_0 and $f_0 + f_p$, respectively, $G_{\max}$ is the simulated maximum gain. The parameters $w_1 \sim w_4$ are weighting factors for each term.

3. APPLICATIONS AND RECEIVER STRUCTURE

As analyzed in Section 2, the proposed electronic beam steering technique is realized at the first sidebands. When the beam at $f_0 + f_p$ is in the direction of θ_0, the beam at $f_0 - f_p$ will be pointing at $2\theta_{f_0} - \theta_0$, simultaneously, where θ_{f_0} is the direction of the beam at f_0. Consequently, there are three beams at f_0 and $f_0 \pm f_p$ which can be used to receive far-field signals arriving from $\theta = \theta_{f_0}$, θ_0 and $2\theta_{f_0} - \theta_0$.

A possible receiver structure based on TMLA for the proposed electronic beam steering is given in Fig. 2. Each element in the array is connected to a RF switch. The RF switches are controlled by a controller such as a digital complex programmable logic device (CPLD) or a signal processing unit, which can be programmed for generating specific time sequences. Due to the time modulation, the output signal of duplexer consists of center frequency and many sidebands at multiples of the time modulation frequency. The Local Oscillator (LO) is used to generate three types of local signal with frequency of $f_0 - f_p - f_I$, $f_0 - f_I$, and $f_0 + f_p - f_I$. After being down converted, the

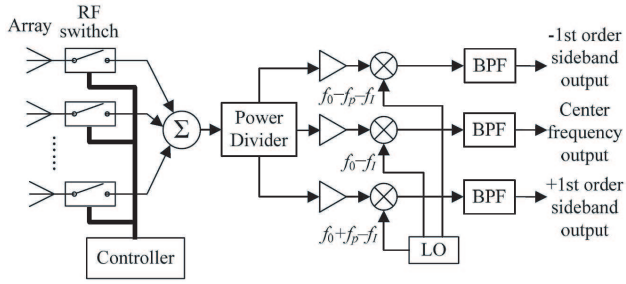

Figure 2. Scheme of a potential receiver structure based on the beam steered TMLA.

received signals at $f_0 \pm f_p$ and at f_0 are all in the same IF stage and band-pass filters (BPFs) with passband at f_I can be used to extract corresponding signals. According to [14, 15], when the time modulation frequency f_p is equal to or greater than the bandwidth of received signal, the center frequency signal and $\pm$1st order sideband signals can be separated and drawn by using BPF. Moreover, the center frequency signal and both first sideband signals contain the same information of the original signal. In order to explain the application of the proposed approach easily and comprehensibly, the discussions on the application associated with some simulation results will be shown in Section 4.2.

4. NUMERICAL AND EXPERIMENTAL RESULTS

To validate the proposed electronic beam steering technique in the TMLA, an S-band 8-element linear array with the center frequency $f_0 = 3.25\,\text{GHz}$ and $\lambda/2$ space between elements was used. The element used in the array is a printed dipole with a double-layered structure. The measured cross-polarization level of this printed dipole antenna was less than $-30\,\text{dB}$ within the frequency band and the measured gain is about $6.5\,\text{dBi}$ at $f_0 = 3.25\,\text{GHz}$ [16].

The feed network was composed of a power divider, digital attenuators, digital phase shifters and high speed RF switches. The digital attenuators and digital phase shifters are used to adjust the excitations such that the static amplitude and phase distribution are uniform. The commercial single-pole-single-throw absorptive RF switch has a switching speed of less than 6ns and the isolation is better than $70\,\text{dB}$. A CPLD card was used to generate the required time sequences to control the high-speed RF switches and the time modulation frequency is set to be $f_p = 0.1\,\text{MHz}$ in the experiment. The entire control box includes the RF feed network, CPLD card and a DC power supply.

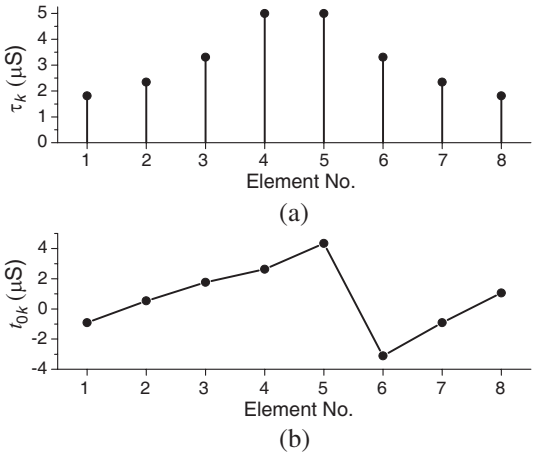

Figure 3. (a) Duration of "on" times τ_k for a -20 dB SLL discrete Taylor pattern ($\bar{n} = 3$) at $f_0 + f_p$; (b) Switch-on time instant t_{0k} for $\theta_0 = +20°$ at $f_0 + f_p$.

Table 1. Comparison of the simulated and measured results of a -20 dB SLL discrete Taylor pattern without DE optimization ($\theta_0 = 20°$).

	Simulated Results					Measured Results				
	SLL	Gain	Relative level (dB)			SLL	Gain	Relative level (dB)		
	(dB)	(dBi)	θ = 0°	θ = 20°	θ = –20°	(dB)	(dBi)	θ = 0°	θ = 20°	θ = –20°
f_0	–18.3	5.4	0	–26.7	–26.7	–17.5	5.0	0	–25.8	–25.8
$f_0 + f_p$	–20	3.3	–25.1	–2.1	–25.6	–19.3	3.2	–28.2	–1.8	–24.3
$f_0 - f_p$	–20	3.3	–25.1	–25.6	–2.1	–19.2	3.1	–25.2	–31.7	–1.9

4.1. Simulated and Measured Patterns

In the first example, the TMLA with uniform excitations was used to realize a -20 dB SLL discrete Taylor ($\overline{n} = 3$) pattern at $f_0 + f_p$ and the desired beam points at $\theta_0 = 20°$, and the beam at f_0 is at 0°. The normalized duration of "on" times ξ_k and the normalized switch-on time instant υ_k can be obtained by using (8) and (9), respectively. Fig. 3 shows the time modulation parameters τ_k and t_{0k}. The simulated and measured patterns at f_0 and $f_0 \pm f_p$ are shown in Fig. 4. It is observed from Fig. 4(a) that the mainlobe of the pattern at f_0 is in the direction of $\theta_0 = 0°$. In Fig. 4(b), the beam at $f_0 + f_p$

points at $\theta_0 = 20°$, while the beam at $f_0 - f_p$ is in the direction of $\theta_0 = -20°$, which is in agreement with the analysis in Section 2. The simulated and measured results such as the SLL, gain and relative level of sidebands are shown in Table 1. Obviously, the measured SLLs and gains are nearly the same as the simulated results. However, there are disagreement between some simulated relative levels of sideband beams and measured data due to the mutual coupling effect and errors of amplitude and phase excitations.

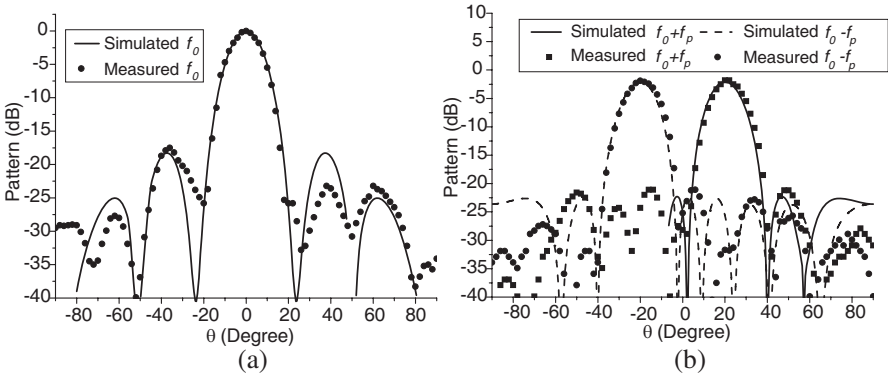

Figure 4. Simulated and measured patterns with the time parameters shown in Fig. 3. (a) Patterns at $f_0 = 3.25\,\text{GHz}$. (b) Patterns at $f_0 \pm f_p$.

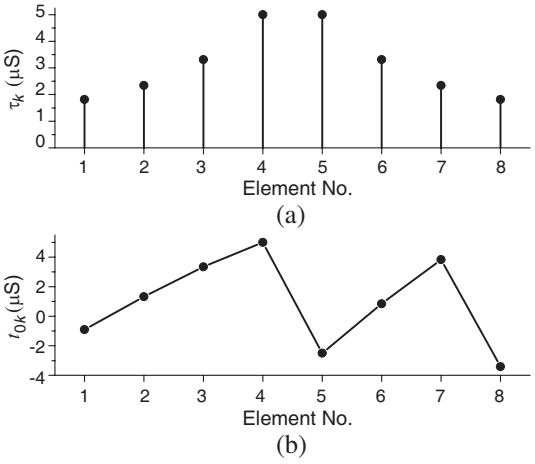

Figure 5. (a) Duration of "on" times τ_k for a $-20\,\text{dB}$ SLL discrete Taylor pattern ($\overline{n} = 3$) at $f_0 + f_p$; (b) Switch-on time instant t_{0k} for $\theta_0 = +30°$ at $f_0 + f_p$.

Table 2. Comparison of the simulated and measured results of a −20 dB SLL discrete Taylor pattern without DE optimization ($\theta_0 = 30°$).

	Simulated Results					Measured Results				
	SLL	Gain	Relative level (dB)			SLL	Gain	Relative level (dB)		
	(dB)	(dBi)	θ = 0°	θ = 30°	θ = −30°	(dB)	(dBi)	θ = 0°	θ = 30°	θ = −30°
f_0	−18.3	5.4	0	−23.7	−23.7	−17.3	4.9	0	−27.5	−20.6
$f_0 + f_p$	−20	3.3	−60.6	−2.1	Null	−19.5	3.2	−24.7	−1.7	−32.9
$f_0 - f_p$	−20	3.3	−60.6	Null	−2.1	−20.1	3.0	−23.8	−25.8	−1.9

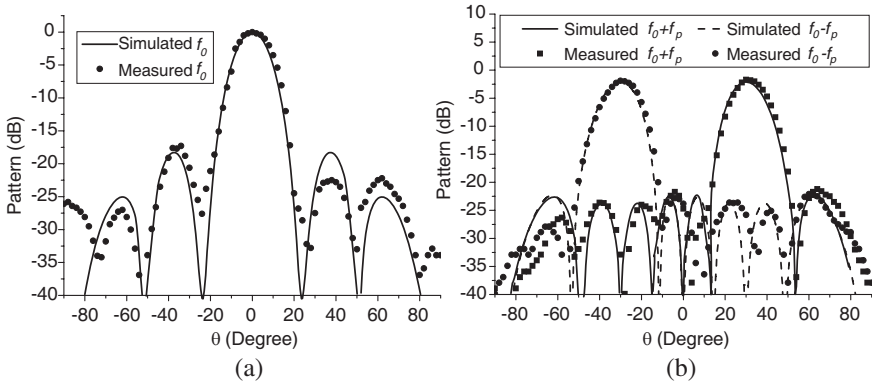

Figure 6. Simulated and measured patterns with the time parameters shown in Fig. 5. (a) Patterns at $f_0 = 3.25$ GHz. (b) Patterns at $f_0 \pm f_p$.

In the second example, the beam at f_0 is also at 0° and the desired pattern at $f_0 + f_p$ is the same as that in the first example, however, the desired beam pointing is at $\theta_0 = 30°$. The time modulation parameters τ_k and t_{0k} are shown in Fig. 5. As compared to Fig. 3, it is apparently noted that τ_k in the two examples are the same due to that the SLLs of the patterns at$f_0 + f_p$ are not changed. On the other hand, the beam steering at $f_0 + f_p$ can be carried out by only adjusting t_{0k}. The simulated and measured patterns at f_0 and $f_0 \pm f_p$ are shown in Fig. 6. Due to the fact that τ_k are not changed, the simulated pattern at f_0 shown in Fig. 6(a) is the same as that in Fig. 4(a). In Fig. 6(b), it is observed that the beam at $f_0 + f_p$ points at $\theta_0 = 30°$, while the beam at $f_0 - f_p$ is in the direction of $\theta_0 = -30°$. Some simulated and measured results are shown in Table 2. The measured SLLs and gains are still in good agreement with simulated results. However, for the same reason such as mutual coupling effect and excitation errors,

there are also some disagreement between simulated relative levels of sidebands and measured results.

In the third example, the DE algorithm is applied to suppress the SLLs of the patterns at both f_0 and $f_0 + f_p$ and to improve the gain of the array. The TMLA is also excited with uniform static amplitude and phase distribution, thus 8 variables need to be optimized. The search ranges for the normalized duration of "on" times ξ_k are selected as $[0, 0.5]$. A -20 dB SLL target is to be realized at f_0 and $f_0 + f_p$, and the desired beam pointing directions at $f_0 + f_p$ is also set to be $\theta_0 = 30^\circ$ and the beam at f_0 is also at 0°. Fig. 7 demonstrates the optimized switch-on time sequences where the shaded parts indicate that the RF switch is on. The corresponding simulated and measured patterns at f_0 and $f_0 \pm f_p$ are shown in Fig. 8. It is observed that the SLLs of the simulated patterns at f_0 and $f_0 \pm f_p$ are all lower than -20 dB and the beam steering at $\theta_0 = 30^\circ$ are carried out at $f_0 + f_p$. Some simulated and measured results are given in Table 3. As compared to the results in Table 2, the gain optimized by the DE algorithm at f_0 has almost 1.0 dB improvement than that in Table 2. However, the gains at $f_0 \pm f_p$ are not increased obviously and the first SBL is lower than that in Table 2.

Table 3. Comparison of the simulated and measured results of a -20 dB SLL pattern with DE optimization ($\theta_0 = 30^\circ$).

	Simulated Results					Measured Results				
	SLL	Gain	Relative level (dB)			SLL	Gain	Relative level (dB)		
	(dB)	(dBi)	θ = 0º	θ = 30º	θ = –30º	(dB)	(dBi)	θ = 0º	θ = 30º	θ = –30º
f_0	–20	6.5	0	–21.0	–21.0	–20.7	6.0	0	–22.4	–28.4
$f_0 + f_p$	–20	3.4	–24.9	–3.1	–24.2	–19.4	3.2	–25.9	–2.8	–26.4
$f_0 - f_p$	–20	3.4	–24.9	–24.2	–3.1	–19.4	3.0	–23.7	–22.6	–3.0

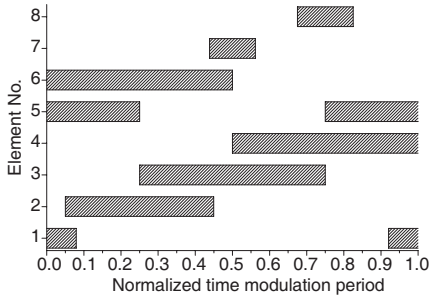

Figure 7. Switch-on time sequences in a normalized time modulation period optimized by DE algorithm.

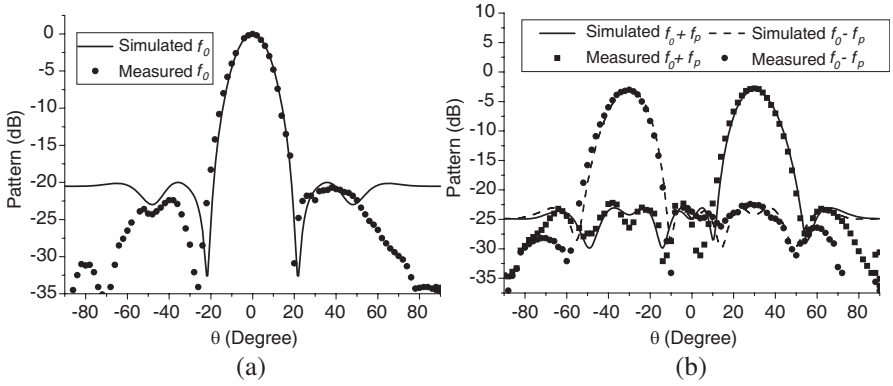

Figure 8. Simulated and measured patterns with the time sequences shown in Fig. 7. (a) Patterns at $f_0 = 3.25\,\text{GHz}$. (b) Patterns at $f_0 \pm f_p$.

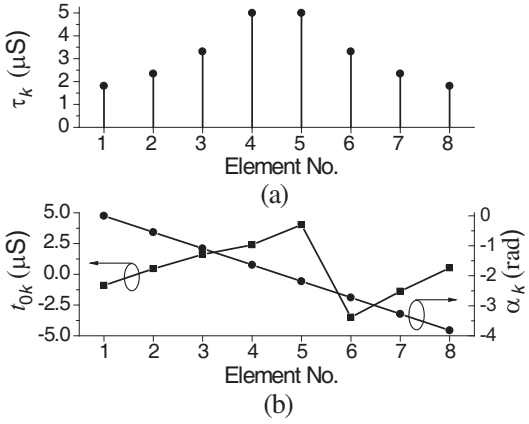

Figure 9. (a) Duration of "on" times τ_k for a $-20\,\text{dB}$ SLL discrete Taylor pattern ($\overline{n} = 3$) at $f_0 + f_p$; (b) Switch-on time instant t_{0k} and static phase excitation α_k for $\theta_{f_0} = 10^\circ$ at f_0 and $\theta_0 = +30^\circ$ at $f_0 + f_p$.

In order to explore more on this approach, the forth example is supplied to demonstrate the relationship of directions of the beams at f_0 and $f_0 \pm f_p$ when the beam at f_0 is not at 0°, where the simulated results are presented. Suppose that the direction of the beam at f_0 is $\theta_{f_0} = 10^\circ$, an $-20\,\text{dB}$ SLL Taylor ($\overline{n} = 3$) pattern at $f_0 + f_p$ is synthesized where the mainlobe is at $\theta_0 = +30^\circ$. The static phase excitation α_k, the time modulation parameters τ_k and t_{0k} are plotted in Fig. 9. The simulated patterns at f_0 and $f_0 \pm f_p$ are shown in

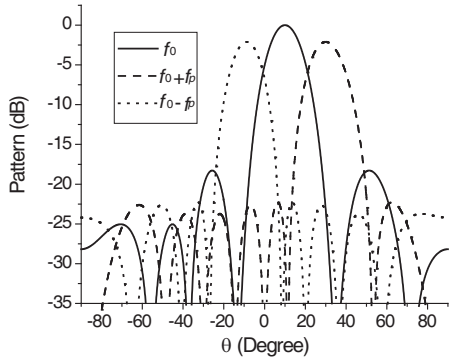

Figure 10. Simulated patterns with the time sequences and static phase excitation shown in Fig. 9.

Fig. 10. It is observed in Fig. 10 that the -20 dB SLL Taylor pattern at $f_0 + f_p$ is realized. Furthermore, the beams at f_0 and $f_0 \pm f_p$ are at 10° and 30°, respectively, and the beam at $f_0 - f_p$ is at -10°, which is in agreement with the analysis in Section 2.

4.2. Simulation on The Received BPSK Modulated Signals

As discussed in Section 3, the beams at the center frequency f_0 and two first sidebands $f_0 \pm f_p$ can be used to receive signals arriving from different directions. Firstly, suppose that there are three far-field BPSK modulated signals arriving from $\theta = 0^\circ$ and $\pm 20^\circ$, respectively, with the same power and carrier frequency $f_0 = 3.25$ GHz impinging on the TMLA with the time sequences shown in Fig. 3. The bandwidth of the BPSK modulated signals are all $B = 0.1$ MHz but they have different code information. The time modulation frequency f_p is equal to B. As shown in Fig. 4, the BPSK modulated signal at $\theta = 20^\circ$ can be received by the mainlobe of the pattern at $f_0 + f_p$, and the BPSK modulated signals at $\theta = 0^\circ$ and $\theta = -20^\circ$ can be suppressed at $f_0 + f_p$ due to that they are received by the sidelobe of the pattern at $f_0 + f_p$. For the same reason, the signals at $\theta = \pm 20^\circ$ can be suppressed at f_0, and the signals at $\theta = +20^\circ$ and $\theta = 0^\circ$ can be suppressed at $f_0 - f_p$. The simulated bit error rates (BERs) of the received BPSK signals at the center frequency and $\pm$1st sideband versus signal-to-noise ratio (SNR) are shown in Fig. 11. It can be observed that the original code information can be obtained after demodulating received BPSK signals when SNR is greater than -5 dB.

Finally, it should point out that the scanning range of the three beams at f_0 and $f_0 \pm f_p$ will be limited in $[-60^\circ, 60^\circ]$ in practical

phased arrays. Thus, three conditions $|\theta_{f_0}| < 60°$, $|\theta_0| < 60°$, and $|\theta_{f_0} - \theta_0| < 60°$ should be satisfied simultaneously. However, the direction of the beam at $f_0 - f_p$ is not independent of that at $f_0 + f_p$. Thus, it would be more universal of using the beams at f_0 and $f_0 + f_p$ than using the three beams and the three conditions can be reduced into two conditions, namely, $|\theta_{f_0}| < 60°$, $|\theta_0| < 60°$.

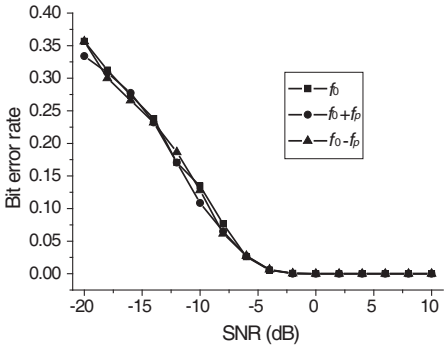

Figure 11. Simulated BERs versus SNR of three BPSK modulated signals arriving from $\theta = 0°$ and $\theta = \pm 20°$ received by the TMLA with time sequences shown in Fig. 3.

5. CONCLUSION

A novel electronic beam steering technique based on the TMLA is proposed in this paper. By controlling only the switch-on time sequences of each element in the antenna array, pattern synthesis and electronic beam steering can be realized at the first sidebands simultaneously without using phase shifters in the array. An *S*-band 8-element linear array was used in the experiment to verify the technique. At the first positive sideband, -20 dB SLL Taylor patterns with the beam steering at $\theta_0 = 20°$ and $\theta_0 = 30°$ were successfully carried out in the experiment, respectively. In addition, the DE algorithm was employed to suppress the SLLs at the center frequency and the first sidebands and to improve the gain simultaneously. The measured gain at the center frequency is 6.3 dBi, which is about 1.0 dB higher than that without DE optimization. The gain at the first positive sideband is about 3.1 dBi when the beam is steered to $\theta_0 = 30°$. Experimental results are in good agreement with the numerical data, thus confirming the proposed beam steering technique in time modulated antenna arrays. The application of the proposed technique can be found in scenarios where the beams at the center

frequency and two first sidebands can be used to receive signals arriving from different directions. The simulation results on receiving BPSK modulated signals arriving from different directions validate the application of the proposed approach.

ACKNOWLEDGMENT

This work was supported in part by the Natural Science Foundation of China under Grant No. 60971030, the New Century Excellent Talent Program in China (Grant No. NCET-06-0809), and in part by the 111 project of China (Grant No. B07046).

REFERENCES

1. Kummer, W. H., A. T. Villeneuve, T. S. Fong, and F. G. Terrio, "Ultra-low sidelobes from time-modulated arrays," *IEEE Trans. Antennas Propagat.*, Vol. 11, No. 5, 633–639, November 1963.
2. Yang, S., Y. B. Gan, and A. Qing, "Sideband suppression in time-modulated linear arrays by the differential evolution algorithm," *IEEE Antennas Wireless Propagat. Lett.*, Vol. 1, 173–175, 2002.
3. Yang, S., Y. B. Gan, and P. K. Tan, "Comparative study of low sidelobe time modulated linear arrays with different time schemes," *Journal of Electromagnetic Waves and Applications*, Vol. 18, No. 11, 1443–1458, 2004.
4. Yang, S., Y. B. Gan, A. Qing, and P. K. Tan, "Design of a uniform amplitude time modulated linear array with optimized time sequences," *IEEE Trans. Antennas Propagat.*, Vol. 53, No. 7, 2337–2339, July 2005.
5. Fondevila, J., J. C. Brégains, F. Ares, and E. Moreno, "Application of time modulation in the synthesis of sum and difference patterns by using linear arrays," *Microwave. Opt. Technol. Lett.*, Vol. 48, No. 5, 829–832, May 2006.
6. Shanks, H. E., "A new technique for electronic scanning," *IEEE Trans. Antennas Propagat.*, Vol. 9, No. 2, 162–166, March 1961.
7. Tennant, A. and B. Chambers, "A two-element time-modulated array with direction-finding properties," *IEEE Antennas Wireless Propagat. Lett.*, Vol. 6, 64–65, 2007.
8. Yang, S., Y. B. Gan, and P. K. Tan, "Evaluation of directivity and gain for time modulated linear antenna arrays," *Microwave. Opt. Technol. Lett.*, Vol. 42, No. 2, 167–171, July 2004.
9. Qing, A., "Electromagnetic inverse scattering of multiple two-dimensional perfectly conducting objects by the differential

evolution strategy," *IEEE Trans. Antenna Propagat.*, Vol. 51, No. 6, 1251–1262, June 2003.

10. Chen, Y., S. Yang, and Z. Nie, "The application of a modified differential evolution strategy to some array pattern synthesis problems," *IEEE Trans. Antennas Propagat.*, Vol. 56, No. 7, 1919–1927, July 2008.
11. Shahoei, H., H. Ghafoori-Fard, and A. Rostami, "A novel design methodology of multiclad single mode optical fiber for broadband optical networks," *Progress In Electromagnetics Research*, PIER 80, 253–275, 2008.
12. Panduro, M. A. and C. Del Rio Bocio, "Design of beam-forming networks for scannable multi-beam antenna arrays using CORPS," *Progress In Electromagnetics Research*, PIER 84, 173–188, 2008.
13. Li, J.-Y. and J. L. Guo, "Optimization technique using differential evolution for Yagi-Uda antennas," *Journal of Electromagnetic Waves and Applications*, Vol. 23, No. 4, 449–461, 2009.
14. Brégains, J. C., J. Fondevila-Gómez, G. Franceschetti, and F. Ares, "Signal radiation and power losses of time-modulated arrays," *IEEE Trans. Antennas Propagat.*, Vol. 56, No. 6, 1799–1804, June 2008.
15. Li, G., S. Yang, Z. Zhao, and Z. Nie, "A study of AM and FM signal reception of time modulated linear antenna arrays," *Progress In Electromagnetics Research Letter*, Vol. 7, 171–181, 2009.
16. Zhou, Z., S. Yang, and Z. Nie, "A novel broadband printed dipole antenna with low cross-polarization," *IEEE Trans. Antenna Propagat.*, Vol. 55, No. 11, 3091–3093, November 2007.